

MAPGD: Multi-Agent Prompt Gradient Descent for Collaborative Prompt Optimization

Yichen Han

South China Normal University
Guangzhou, China
2024024502@m.scnu.edu.cn

Zhengpeng Zhou

Shanghai Jiaotong University
Shanghai, China
alex_chou@sjtu.edu.cn

Yang Yang

Silicon Sapiens LLC
Jinan, China
yang@esapiens.ai

Yunyan Zhang

Silicon Sapiens LLC
Jinan, China
yunyan@fangyingmobile.com

Yuhang Han

Northwestern Polytechnical
University
Xi'an, China
hanyh@mail.nwp.edu.cn

Guanyu Liu

University of Macau
Macau, China
dc32352@um.edu.mo

Wenli Wang

Silicon Sapiens LLC
Jinan, China
wenli@esapiens.ai

Lewei He*

South China Normal University
Guangzhou, China
helewei@m.scnu.edu.cn

Bojun Liu

University of Sydney
Sydney, Australia
liubojun9999@gmail.com

Zeng Zhang

South China Normal University
Guangzhou, China
2024024588@m.scnu.edu.cn

Isaac N Shi

Silicon Sapiens LLC
Jinan, China
isaac@goldensection.com

Tianyu Shi†

University of Toronto
Toronto, Canada
tys@cs.toronto.edu

ABSTRACT

Prompt engineering is essential for fully leveraging large language models (LLMs), yet existing optimization methods often follow a single trajectory, leading to limited adaptability, gradient conflicts, and high computational overhead. We propose MAPGD (Multi-Agent Prompt Gradient Descent), a novel framework that reconceptualizes prompt optimization as a collaborative multi-agent process. MAPGD incorporates specialized agents focusing on orthogonal refinement dimensions—such as instruction clarity, example selection, format structuring, and stylistic adaptation—and coordinates their contributions through semantic gradient embedding, conflict detection, and fusion. To further enhance robustness and stability, MAPGD proposes two new mechanisms: Hypersphere-Constrained Gradient Clustering (HCGC), which enforces angular margin constraints to ensure intra-cluster compactness and inter-cluster separation, and Channel-Adaptive Agent Weighting (CAAW), which dynamically reweights agent contributions based on validation performance. Experiments on classification and reasoning benchmarks demonstrate that MAPGD consistently outperforms single-agent and random baselines in both accuracy and efficiency. Ablation studies validate the effectiveness of gradient fusion, agent specialization, and conflict resolution. Together, these contributions establish MAPGD as a unified, gradient-inspired, and interpretable framework for robust prompt optimization with theoretical convergence guarantees.

CCS CONCEPTS

- Computing methodologies → Discourse, dialogue and pragmatics.

KEYWORDS

Prompt Optimization, Multi-Agent Systems, Large Language Models, Gradient Descent

1 INTRODUCTION

Large Language Models (LLMs), trained on vast webscale corpora, have recently demonstrated remarkable generalization capabilities across diverse natural language processing (NLP) tasks [1, 4]. A central factor influencing their performance is the design of prompts, which serve as the primary interface for guiding model behavior. However, prompt construction remains largely a manual, trial-and-error process that demands substantial human labor [15] and domain expertise [27, 35]. This inefficiency highlights the urgent need for automatic or semi-automatic strategies to systematically generate or refine prompts. Such approaches can reduce manual burden, improve task performance, and provide interpretable optimization pathways.

Recent research has explored this problem through two primary directions. One line of work introduces auxiliary models or differentiable prompt embeddings to approximate gradient-based optimization [9, 26]. Yet, these methods often assume access to the internal states or parameters of LLMs [16, 30], which is impractical in real-world API-only scenarios. Another line of work employs reinforcement learning or feedback-driven editing to discretely manipulate prompts [36, 37]. While effective in some cases, these

*Corresponding author.

†Corresponding author.

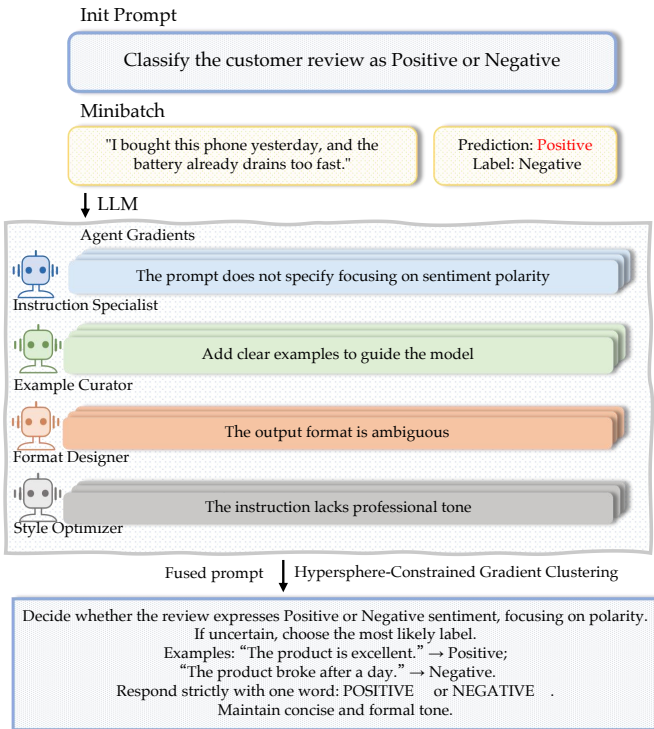


Figure 1: Overview of the Multi-Agent Prompt Gradient Descent for Collaborative Prompt Optimization.

algorithms may produce incoherent prompts, incur high computational costs, or rely on unguided Monte Carlo search over the semantic space. Collectively, these limitations highlight the need for more robust, interpretable, and scalable frameworks for prompt optimization.

Addressing this gap, Pryzant et al. [25] proposed ProTeGi, a non-parametric approach that mirrors gradient descent in textual space. ProTeGi generates natural language “gradients” from model errors and iteratively edits prompts in semantically opposite directions. To balance exploration and exploitation, it further integrates beam search and bandit-based candidate selection, achieving significant gains over earlier baselines. Nevertheless, ProTeGi operates under a single-agent paradigm, which restricts the diversity of optimization signals and leaves unresolved conflicts among competing refinement directions.

To overcome these limitations, we propose MAPGD (Multi-Agent Prompt Gradient Descent), a novel framework that reconceptualizes prompt optimization as a collaborative multi-agent process (Figure 1). MAPGD introduces a set of specialized agents, each dedicated to distinct refinement dimensions—such as instruction clarity, example selection, format structuring, and stylistic adaptation. To reconcile heterogeneous improvement signals, MAPGD employs a semantic gradient coordinator that embeds textual gradients into a shared vector space, enabling conflict detection, clustering, and fusion. In addition, we propose two novel mechanisms to further enhance robustness and stability: Hypersphere-Constrained Gradient Clustering (HCGC), which introduces angular margin constraints on

the unit hypersphere to ensure compact intra-cluster coherence and inter-cluster separation, and Channel-Adaptive Agent Weighting (CAAW), which dynamically reweights agent contributions according to validation performance, amplifying effective optimization channels while suppressing noisy ones. Together, these innovations endow MAPGD with improved robustness, stability, and interpretability, enabling it to consistently outperform single-agent baselines such as ProTeGi across diverse optimization scenarios.

Beyond empirical improvements, MAPGD also provides a theoretical foundation for convergence. Under mild stochastic approximation assumptions, we prove that the multi-agent gradient coordination and fusion mechanisms preserve the convergence properties of classical gradient descent, yielding almost sure convergence to a local optimum at a sublinear rate of $O(1/\sqrt{T})$, where T denotes the number of iterations. This result establishes that, despite operating in a discrete, textual prompt space and coordinating multiple heterogeneous agents, MAPGD maintains stable and predictable optimization dynamics, bridging practical prompt refinement with rigorous theoretical guarantees.

2 RELATED WORK

Prompt Learning and Optimization. Early efforts relied on manual engineering, which lacks scalability. Automated methods include reinforcement learning [9], evolutionary search [12], and Bayesian optimization [28]. Continuous prompt tuning (e.g., prefix tuning [17], soft prompts [16]) optimizes embeddings but sacrifices interpretability. MAPGD instead pursues interpretable natural language optimization with structured feedback.

Multi-Agent Collaboration. Multi-agent systems are well-studied in RL, distributed AI, and game theory. In NLP, multi-agent debate [10, 18], cooperative reasoning, and collaborative generation [13] show that role specialization outperforms monolithic optimization. MAPGD applies this principle by assigning agents to distinct prompt dimensions and coordinating them via gradient fusion.

Gradient-Inspired Optimization. ProTeGi [25] and similar approaches approximate prompt gradients through self-feedback. While effective, single-agent descent struggles with limited signal diversity and inherent conflict resolution challenges [34]. A monolithic agent can generate self-contradictory pseudo-gradients, as different refinement dimensions are not explicitly disentangled. For instance, to correct a misclassification, a single agent might propose a gradient to add more illustrative examples, while an implicit counter-gradient aims to make the instructions more concise. This creates a direct conflict in prompt length and structure, potentially leading to suboptimal or oscillating optimization trajectories. MAPGD extends this paradigm by embedding gradients semantically, explicitly detecting such conflicts, and fusing them coherently through LLM-driven synthesis.

Geometric and Adaptive Mechanisms. Contrastive learning and angular margin constraints are effective in representation learning. Wang and Isola formalize how contrastive losses enforce *alignment* and *uniformity*, providing a theoretical lens [32]. This principle of hyperspherical separation to enhance discriminability spans domains. In face recognition, margin-based softmax losses such as SphereFace [21], CosFace [31], and ArcFace [8] enforce angular

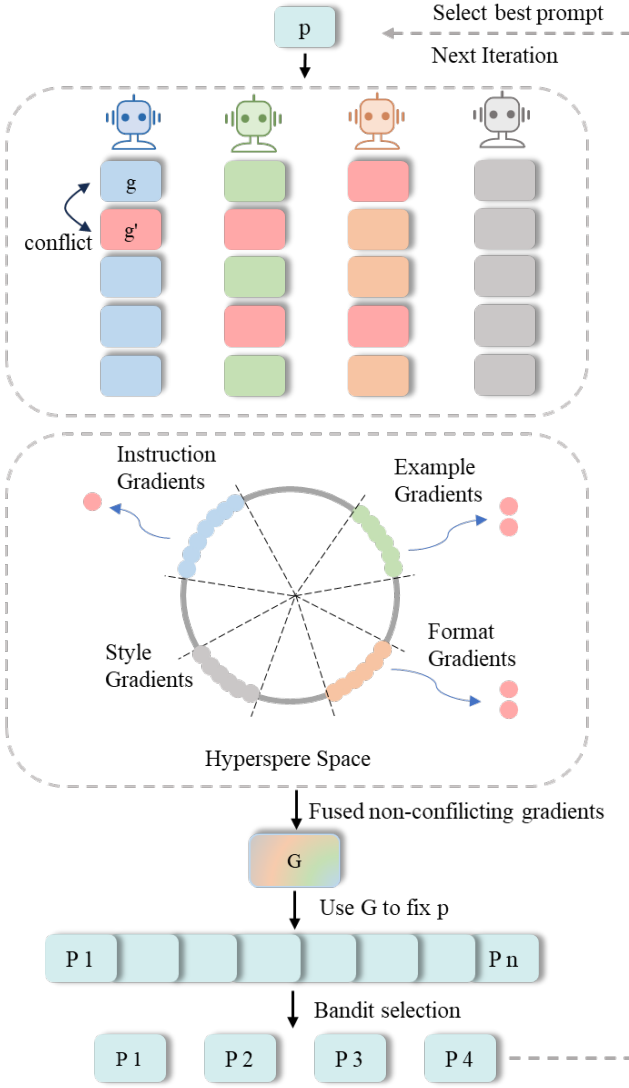


Figure 2: Workflow of MAPGD. Starting from an initial prompt p , specialized agents propose diverse pseudo-gradients $\{g, g', g'', g''', \dots\}$ (top). These gradients are semantically embedded and projected onto the unit hypersphere, then clustered with angular-margin constraints to form coherent groups (middle). Clustered directions are fused via LLM-driven synthesis into composite gradients G , which generate refined candidate prompts $\{P_1, P_2, \dots, P_n\}$ (bottom). The best candidates are iteratively selected and fed back to continue the prompt optimization loop.

margins between identities. Chen et al. [6] introduce a distance polarization regularizer for large-margin contrastive learning, pushing inter-cluster samples apart while keeping intra-cluster representations tight. Inspired by these advances, our Hypersphere-Constrained Gradient Clustering (HCGC) enforces intra-cluster compactness and inter-cluster separation for semantic gradients,

complemented by Channel-Adaptive Agent Weighting (CAAW) adjusting agent contributions. Together, these modules enhance multi-agent gradient descent with geometry-aware clustering and adaptive coordination.

In summary, MAPGD unifies prompt learning, multi-agent collaboration, gradient descent, and geometry-inspired optimization into a scalable and interpretable framework.

3 METHODOLOGY

3.1 Framework Overview

MAPGD formulates prompt optimization as a hybrid discrete–continuous gradient descent process in the natural language space. Unlike continuous embedding–based methods such as prefix or soft prompt tuning [16, 17], MAPGD explicitly manipulates interpretable textual prompts while leveraging gradient-inspired feedback for iterative refinement (Figure 2).

At each iteration, specialized agents analyze misclassified or suboptimal examples and produce pseudo-gradients in natural language. These gradients are semantically embedded, clustered, and adaptively fused to mitigate conflicts and ensure coherent optimization. The resulting fused gradients are applied to generate successor prompts, which are then evaluated and filtered under limited budgets. Iterative repetition yields a dynamically evolving prompt trajectory that balances exploration of diverse directions with exploitation of promising refinements.

Formally, the optimization objective is defined as:

$$F(p) = \mathbb{E}_{(x,y) \sim \mathcal{D}} [\ell(M(x; p), y)], \quad (1)$$

where $\ell(\cdot, \cdot)$ denotes a task-specific loss function. The goal is:

$$p^* = \arg \min_p F(p). \quad (2)$$

Unlike stochastic gradient descent (SGD), where gradients are continuous, MAPGD constructs textual pseudo-gradients:

$$\nabla F(p^{(t)}) \approx g^{(t)}, \quad (3)$$

which act as semantic analogues of numerical gradients.

3.2 Specialized Prompt Agents

Each agent specializes in a distinct dimension of prompt optimization, analogous to orthogonal gradient directions. For example: A_1 : instruction clarity (g_1), A_2 : example selection (g_2), A_3 : format specification (g_3), A_4 : stylistic refinement (g_4), and optionally a generic agent for broad improvements. At iteration t , the gradient set is:

$$G^{(t)} = \{g_1^{(t)}, g_2^{(t)}, \dots, g_K^{(t)}\}.$$

This decomposition supports parallel exploration of diverse refinements, alleviating local minima issues inherent in single-agent approaches.

3.3 Hypersphere-Constrained Gradient Clustering

Inspired by hyperspherical contrastive learning [21, 31], our HCGC mechanism is designed to enhance the semantic consistency of multi-agent gradients by enforcing intra-cluster compactness and inter-cluster separation in a normalized hypersphere space. This approach addresses the challenge of conflicting pseudo-gradients

generated by heterogeneous agents, ensuring that semantically coherent optimization directions are emphasized while contradictory ones are disentangled. The overall process and the geometric intuition of our method are illustrated in Figure 3.

Gradient Embedding on Hypersphere. Given a set of agent-generated gradients $G^{(t)} = \{g_1^{(t)}, g_2^{(t)}, \dots, g_K^{(t)}\}$, each gradient is encoded into a d -dimensional vector $v_k^{(t)} = \phi(g_k^{(t)})$, where ϕ denotes a pre-trained language encoder. For this purpose, we utilize a Sentence Transformer model, such as all-MiniLM-L6-v2, which provides compact and semantically informative embeddings. To eliminate scale variance, we normalize each embedding onto the unit hypersphere:

$$\hat{v}_k^{(t)} = \frac{v_k^{(t)}}{\|v_k^{(t)}\|}, \quad \hat{v}_k^{(t)} \in \mathbb{S}^{d-1}. \quad (4)$$

The similarity between two gradients is then computed as the cosine similarity. Gradients are considered to be in conflict if their angular distance exceeds a predefined threshold, $\theta_{conflict}$:

$$\text{sim}(\hat{v}_i, \hat{v}_j) = \hat{v}_i^\top \hat{v}_j = \cos(\Delta(\hat{v}_i, \hat{v}_j)), \quad (5)$$

where $\Delta(\cdot, \cdot)$ denotes the angular distance on the hypersphere.

Figure 4 illustrates a concrete example in the sentiment classification task, where different agents generate multiple pseudo-gradients. While some gradients form semantically coherent clusters (intra-cluster compactness), others introduce conflicts that must be separated through angular margin constraints.

Angular Margin Constraint. To mitigate conflicts and ensure clear separation between semantic clusters, HCGC enforces an angular margin constraint on the unit hypersphere. Let \hat{v}_k denote a normalized gradient vector, u_i the centroid of its assigned cluster i , and u_j the centroid of any other cluster j . We define the corresponding angles as

$$\alpha = \Delta(\hat{v}_k, u_i), \quad \beta = \Delta(\hat{v}_k, u_j).$$

A standard clustering assignment only requires $\alpha < \beta$. However, to enforce stronger separation, we introduce a margin scaling factor $n \geq 1$:

$$n \cdot \alpha < \beta.$$

Since $\cos(\theta)$ is monotonically decreasing for $\theta \in [0, \pi]$, this condition is equivalently expressed in terms of cosine similarity:

$$\cos(n \cdot \alpha) > \cos(\beta), \quad n \geq 1. \quad (6)$$

This constraint ensures that \hat{v}_k is not only closer to its own centroid u_i , but also significantly more aligned with it than with any other centroid u_j . Geometrically, as illustrated in Figure 3 (c), this confines \hat{v}_k to a scaled angular neighborhood around u_i , effectively creating a “cone of acceptance” narrower than the standard Voronoi region on the hypersphere. By enforcing this margin, HCGC simultaneously enhances inter-cluster separation and intra-cluster compactness, yielding more stable and reliable gradient fusion. During clustering, any gradient \hat{v}_k violating this condition with respect to some u_j is considered for reassignment to a cluster where the margin holds; otherwise, it remains in its original cluster.

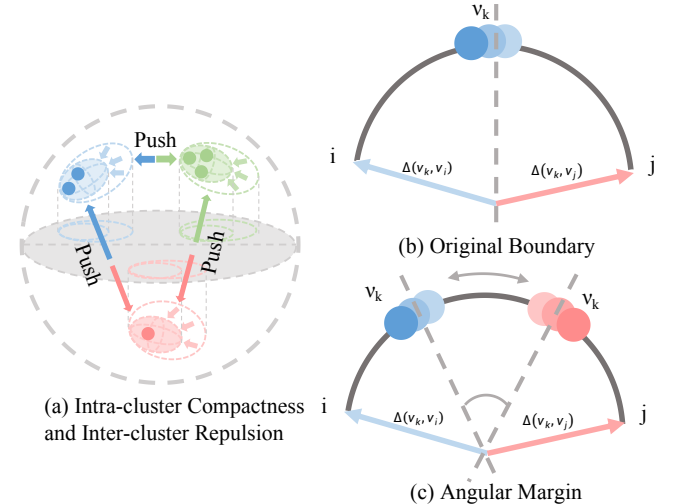


Figure 3: Details of Hypersphere-Constrained Gradient Clustering

Optimization Objective. Analogous to hyperspherical contrastive learning, the clustering objective combines intra-cluster compactness and inter-cluster repulsion:

$$\mathcal{L}_{HCGC} = -\log \frac{\exp(\cos(\Delta(\hat{v}_i, \hat{v}_j))/\tau)}{\sum_{k \in \mathcal{N}(i)} \exp(\cos(\Delta(\hat{v}_i, \hat{v}_k))/\tau)}, \quad (7)$$

where (\hat{v}_i, \hat{v}_j) is a positive pair from the same cluster, $\mathcal{N}(i)$ denotes negatives from other clusters, and τ is a temperature factor. By optimizing \mathcal{L}_{HCGC} , we obtain semantically well-aligned clusters of gradients, ensuring coherent downstream fusion.

After clustering, gradients within each semantically coherent group are fused into a single representative gradient. This fusion is typically performed by an LLM, guided by the original suggestions. To maintain diversity and avoid redundancy among the fused gradients, a semantic diversity filter is applied, discarding suggestions that are too similar to already selected ones, controlled by a diversity threshold $\theta_{diversity}$.

3.4 Channel-Adaptive Agent Weighting

While HCGC ensures structural consistency across gradients, gradients within the same cluster may still differ in reliability due to heterogeneous agent expertise. To address this, we propose Channel-Adaptive Agent Weighting (CAAW), which dynamically calibrates agent contributions according to their historical effectiveness, akin to channel-wise recalibration in neural representations [14].

Adaptive Weight Assignment. Let $s_k^{(t)}$ denote the validation performance gain associated with gradient $g_k^{(t)}$. The adaptive weight of each gradient is computed via a softmax normalization:

$$w_k^{(t)} = \frac{\exp(\lambda s_k^{(t)})}{\sum_{j \in C} \exp(\lambda s_j^{(t)})}, \quad (8)$$

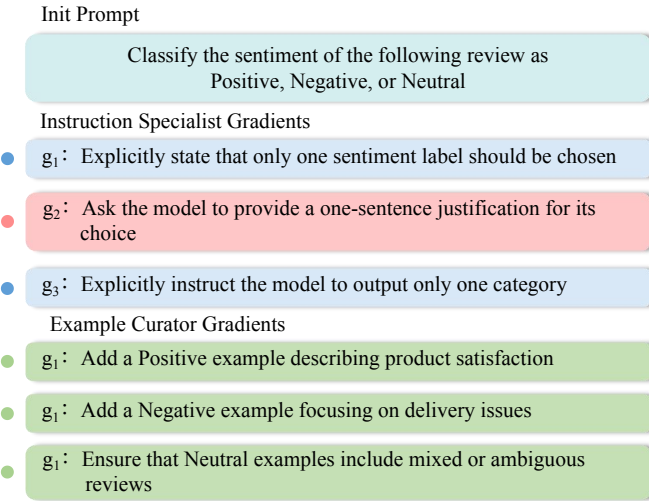


Figure 4: Illustration of agent-generated pseudo-gradients in a sentiment classification task. Blue gradients form a coherent cluster under the Instruction Specialist, while the red gradient represents a conflicting update. Green gradients from the Example Curator constitute another semantically compact cluster. This motivates the need for hypersphere-constrained clustering to enforce intra-cluster compactness and inter-cluster separation.

where C is the current cluster, and λ controls the sharpness of weighting. This formulation emphasizes historically effective agents while down-weighting less reliable ones.

Gradient Fusion. The final fused gradient is expressed as:

$$g_{\text{fused}}^{(t)} = \Psi \left(\sum_{k \in C} w_k^{(t)} g_k^{(t)} \right), \quad (9)$$

where $\Psi(\cdot)$ denotes an LLM-driven synthesis function that integrates multiple textual directions into a coherent refinement.

Robustness and Stability. By recalibrating agent contributions at the channel level, CAAW suppresses redundant or conflicting updates while amplifying stable and discriminative directions. Theoretically, this reduces variance in the optimization trajectory and prevents over-amplification of noisy gradients, thereby ensuring convergence to semantically robust prompt candidates.

3.5 Candidate Generation and Selection

Fused gradients generate successor prompts $\{p'_1, \dots, p'_n\}$. MAPGD applies lightweight filtering and optional bandit-based evaluation [3] to control computational overhead. However, unlike prior work that heavily relies on bandit selection, our framework emphasizes geometry-aware clustering (HCGC) and adaptive agent weighting (CAAW) as the primary mechanisms ensuring robustness and interpretability.

3.6 Theoretical Convergence (Informal)

We provide a convergence analysis of MAPGD in Appendix C. Here we summarize the key assumptions: (i) bounded variance of agent pseudo-gradients, (ii) Lipschitz continuity of the loss function, and (iii) unbiased sampling from bandit-based candidate selection. Under these conditions, MAPGD inherits the convergence properties of stochastic gradient descent and achieves almost sure convergence to a local optimum at a sublinear rate of $\mathcal{O}(1/\sqrt{T})$. Intuitively, HCGC reduces variance by enforcing geometric separation, CAAW emphasizes historically reliable agents, and bandit selection maintains unbiased exploration, together ensuring stable optimization dynamics.

4 EXPERIMENTS

We design comprehensive experiments to evaluate the effectiveness, efficiency, and robustness of the proposed MAPGD framework. To ensure comparability, we reproduce the experimental setup of ProTeGi under identical conditions and extend the evaluation with ablation studies and token consumption analysis. In addition, we include a real-world case study on prompt optimization for text generation (see Appendix D), which highlights the applicability of MAPGD beyond controlled benchmarks.

4.1 Datasets

To ensure comparability with ProTeGi, we evaluate MAPGD on the same four benchmark NLP classification tasks that span diverse domains and languages:

- **Jailbreak** [29]: a novel task to determine whether a user input to an LLM continuation API constitutes a jailbreak attempt. Jailbreak attacks are defined as user strategies that aim to make the model violate its own safety policies, such as generating harmful content or exposing hidden instructions. The dataset contains 1306 multilingual examples with human-annotated jailbreak labels.
- **Ethos** [22]: an English hate speech detection dataset with 997 online comments annotated as hateful or non-hateful.
- **LIAR** [33]: a large-scale dataset for fake news detection, consisting of 4,000 short statements labeled with ground-truth veracity, along with context information.
- **Sarcasm** [11]: an Arabic sarcasm detection dataset with 10,000 online comments, labeled for the presence or absence of sarcasm.

Beyond classification, we further evaluate on three arithmetic reasoning datasets that require multi-step logical inference and symbolic manipulation:

- **GSM8k** [7]: a widely used benchmark of 8,500 grade-school math problems that require step-by-step reasoning.
- **AQUARAT** [20]: a dataset of algebraic word problems designed to test symbolic reasoning and program induction.
- **SVAMP** [23]: a benchmark focusing on simple arithmetic word problems with diverse linguistic variations, serving as a testbed for robustness to paraphrasing.

In addition, we include a real-world text generation case study in the Appendix to highlight MAPGD’s applicability beyond controlled benchmarks.

4.2 Experimental Setup

For each dataset, we randomly sample 50 examples for development and 150 for testing. All reported results are averaged over three independent runs to mitigate variance. The evaluation metric is binary F1 score on the test set, computed by max-pooling over the final beam of candidate prompts.

Unless otherwise stated, all experiments are conducted with the January 2023 version of gpt-3.5-turbo through the Azure OpenAI API. The temperature is set to 0.0 for classification tasks to ensure deterministic predictions.

To ensure a fair comparison, all methods—including baselines and MAPGD—use the same initial prompts, training data, and random seeds. The iteration budget is fixed at $T = 10$ across all experiments. We adopt default parameter values without additional hyperparameter search, to ensure that performance differences are attributable to algorithmic design rather than parameter tuning.

For our MAPGD implementation, we instantiate the framework with specific hyperparameters introduced in Section 3.3. We use the all-MiniLM-L6-v2 Sentence Transformer as the gradient encoder ϕ . The conflict threshold $\theta_{conflict}$ is set to 0.3, and we use a cluster similarity threshold of 0.7 for grouping gradients. The diversity threshold $\theta_{diversity}$ is set to 0.7 to ensure varied candidate prompts. Bandit-based selection adopts a UCB strategy with a budget of 80 evaluations. We set the CAAW weighting parameter λ to 1 (see Appendix A for a sensitivity analysis on different values).

Accordingly, all experiments reported in Section 4.4 were conducted with these modules enabled, unless explicitly ablated.

4.3 Baselines

To evaluate the effectiveness of MAPGD, we compare it against a set of non-parametric prompt optimization methods, following the setup of ProTeGi [25], and additionally include ProTeGi itself as a strong baseline. Specifically, we consider:

- **ProTeGi**: the original prompt gradient descent framework, where a single agent iteratively generates pseudo-gradients and candidate prompts, with bandit-based selection. This serves as our primary baseline for comparison.
- **Monte-Carlo (MC)** [37]: an iterative but directionless Monte Carlo search over the prompt space. For fairness, we match the number of samples per candidate to the successors generated by MAPGD.
- **Reinforcement Learning (RL)** Recent approaches such as GrIPS [24] and TEMPERA [36] formulate prompt optimization as a reinforcement learning problem. In these methods, the prompt text is first segmented into phrases, and the search space is explored via phrase-level edit operations, including addition, paraphrasing, swapping, and deletion.
- **AutoGPT**: an open-source autonomous agent system that improves prompts through self-directed feedback loops. We configure AutoGPT with the same number of examples and errors as MAPGD, running for the same number of optimization steps.

For arithmetic reasoning, we additionally compare against three competitive baselines, all reported with GPT-3.5-Turbo in a zero-shot setting:

- **InsZero** [5]: a zero-shot prompting method with instruction tuning.
- **Instinct** [19]: an instruction-following baseline that improves prompting robustness.
- **PromptWizard** [2]: a state-of-the-art prompt synthesis framework that iteratively enriches prompts with intermediate reasoning steps and examples.

This collection of baselines allows us to evaluate MAPGD not only against single-agent gradient-based optimization, but also against strong arithmetic reasoning methods optimized for chain-of-thought style prompting.

4.4 Experimental Results

Figure 5 summarizes the overall performance across the four benchmark classification datasets. Our results demonstrate that MAPGD consistently achieves the best performance under varying evaluation budgets, outperforming all baselines by a notable margin.

On the Jailbreak dataset, MAPGD attains an average F1 of 0.86, surpassing ProTeGi (0.82) and MC (0.76), while substantially improving over RL (0.67) and AutoGPT (0.62). The improvement margin remains stable across different budgets, reaching up to +5.5% over ProTeGi and +10.9% over MC at 30 evaluations.

For E ethos, MAPGD pushes performance from the strong baseline of 0.93 (p_0) to 0.98, showing a consistent +1.5% advantage over ProTeGi and +4.0% over MC. These improvements highlight MAPGD’s ability to leverage gradient fusion even in relatively saturated tasks.

On the more challenging LIAR dataset, MAPGD achieves 0.71, representing the largest relative gains: +8.0% over ProTeGi, +11.0% over MC, and a substantial +17.0% over the initial prompt. This suggests that multi-agent collaboration and semantic clustering are particularly beneficial in noisy, fact-checking tasks.

For Sarcasm, MAPGD steadily improves from 0.84 (p_0) to 0.91, outperforming ProTeGi (0.87) and MC (0.85). Interestingly, AutoGPT sometimes reduces performance below the initial prompt, echoing earlier findings that unguided agent feedback may destabilize optimization.

Beyond classification, we further evaluate MAPGD on arithmetic reasoning benchmarks, which require detailed multi-step inference. Table 1 compares MAPGD against three strong baselines—InsZero, Instinct, and PromptWizard—on GSM8k, AQUARAT, and SVAMP. MAPGD achieves consistent improvements across all datasets, with particularly notable gains on GSM8k (93.5%), surpassing the previous best by +3.5 points. On AQUARAT and SVAMP, MAPGD reaches 60.3% and 84.1%, respectively, representing stable improvements over the strongest baselines. These results confirm that MAPGD not only excels in classification but also transfers effectively to challenging reasoning tasks.

Overall, MAPGD improves over ProTeGi and MC by 3–7% on average for classification, while maintaining strong gains on arithmetic reasoning datasets. These results validate our hypothesis that multi-agent specialization and hypersphere-constrained clustering provide more robust and adaptive optimization compared to single-agent or rule-based approaches.

Table 1: Arithmetic reasoning accuracy (%) on GSM8k, AQUARAT, and SVAMP. Best results in bold.

Method	GSM8k	AQUARAT	SVAMP
InsZero	74.2	54.3	79.5
Instinct	74.5	54.7	81.0
PromptWizard	90.0	58.2	82.3
MAPGD	93.5	60.3	84.1

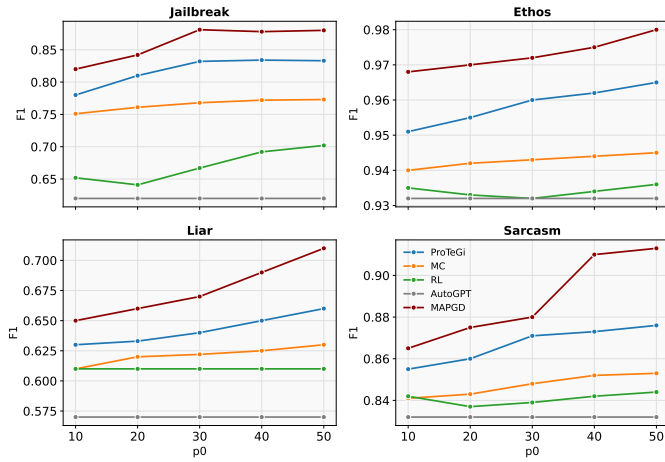


Figure 5: Test performance (F1 score) vs. API query budget per prompt candidate across four benchmark tasks.

4.5 Ablation Study

To precisely attribute the performance gains of MAPGD, we perform a comprehensive ablation study (see Table 2 for the detailed configurations and results). Beyond standard ablation variants (e.g., No Gradient Fusion, Single-Agent Only, No Specialization), we design targeted experiments specifically to isolate the contributions of the two proposed modules HCGC and CAAW, as well as to evaluate resource efficiency and robustness.

Ablation configurations. We evaluate the following variants:

- (1) MAPGD (full): our full method with HCGC and CAAW.
- (2) No Gradient Fusion: disable the fusion stage; agents act independently and their suggestions are applied without semantic clustering.
- (3) Single-Agent Only: only one specialized agent (instruction specialist) is used.
- (4) No Specialization: agent roles are randomized each iteration (no fixed expertise).
- (5) w/o HCGC: keep clustering but remove the hypersphere angular-margin constraint. This reduces to standard K-means clustering with cosine similarity, which acts as an off-the-shelf baseline for comparison.
- (6) w/o CAAW: replace Channel-Adaptive Agent Weighting with simple uniform averaging of agent gradients.

Table 2: Ablation study: classification performance (F1 score, mean \pm std over 3 runs). Best results in bold.

Method	Jailbreak	Ethos	LIAR	Sarcasm
MAPGD (full)	0.88 \pm 0.01	0.98 \pm 0.02	0.71 \pm 0.01	0.91 \pm 0.01
No Gradient Fusion	0.83 \pm 0.02	0.92 \pm 0.02	0.67 \pm 0.02	0.86 \pm 0.02
Single Agent Only	0.80 \pm 0.03	0.87 \pm 0.03	0.62 \pm 0.02	0.82 \pm 0.03
No Specialization	0.80 \pm 0.02	0.90 \pm 0.02	0.65 \pm 0.02	0.84 \pm 0.02
w/o HCGC	0.84 \pm 0.02	0.94 \pm 0.02	0.68 \pm 0.02	0.87 \pm 0.02
w/o CAAW	0.85 \pm 0.02	0.95 \pm 0.02	0.69 \pm 0.02	0.88 \pm 0.02
w/o HCGC + CAAW	0.82 \pm 0.03	0.91 \pm 0.03	0.66 \pm 0.02	0.83 \pm 0.02

Table 3: Token consumption comparison between ProTeGi and MAPGD (averaged over 3 runs). MAPGD achieves lower token usage and higher efficiency.

Metric	ProTeGi	MAPGD (full)
Total Tokens	256k	236k
Calls	962	643
Avg F1	0.83	0.87
F1 / Token ($\times 10^{-6}$)	3.24	3.69

- (7) w/o HCGC+CAAW: use standard K-means clustering with cosine similarity (no angular margin) and replace adaptive weighting with uniform fusion.

4.6 Token Consumption Analysis

To further assess the efficiency of MAPGD, we conducted a dedicated token consumption experiment, following the same setup as in Section 4.2. In this experiment, we recorded the number of tokens used in every API call, where the token cost of a single call is defined as the sum of input tokens and output tokens. For each method, we accumulated token usage across all iterations and runs, and report the total tokens, average tokens per iteration, and total number of LLM calls. In addition, we report performance efficiency as the ratio of average F1 score to total token usage.

Table 3 presents the results, comparing MAPGD with the ProTeGi. MAPGD not only achieves higher F1 scores, but also requires fewer tokens and API calls overall. Specifically, MAPGD reduces the average token cost per iteration from roughly 25.6k to 23.6k, corresponding to a $\sim 8\%$ saving in token usage. At the same time, MAPGD improves the performance-per-token efficiency by more than 10%. These findings indicate that multi-agent collaboration with HCGC and CAAW enables more effective use of query budgets, reducing redundancy while preserving accuracy.

4.7 Agent Number Sensitivity

To better justify the design choice of using four specialized agents, we conduct a sensitivity analysis by varying the number of agents $N \in \{2, 4, 6\}$. For $N = 2$, we retain only the Instruction Specialist and Example Curator; for $N = 6$, we extend the framework with two additional stylistic and format-focused agents. All other settings follow Section 4.2.

Figure 6 shows the average F1 score across the four datasets. We observe that performance improves substantially when moving from $N = 2$ to $N = 4$, confirming the benefit of multi-agent specialization. Increasing to $N = 6$ yields only marginal gains while incurring higher token cost, suggesting diminishing returns. These results indicate that four agents provide a favorable balance between effectiveness and efficiency, validating our default configuration.

Overall, these findings suggest that an excessively small agent set cannot comprehensively capture different prompt dimensions, whereas an overly large set introduces redundancy and potential conflicts. A moderate number of agents, four in our case, provides the best trade-off.

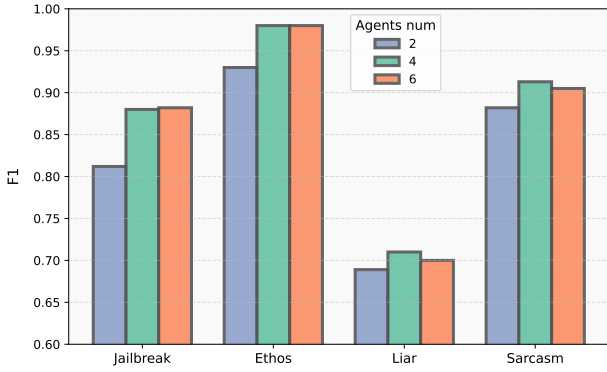


Figure 6: Agent number sensitivity analysis. Increasing agents from 2 to 4 yields clear improvements, while further increasing to 6 brings diminishing returns.

4.8 Experimental Insights

Our experimental evaluation provides several key insights:

- **Effectiveness of multi-agent collaboration.** Across all four benchmark tasks, MAPGD consistently outperforms single-agent ProTeGi and other baselines. The largest gains are observed on LIAR and Jailbreak, where conflicting gradient signals are common. This demonstrates that multi-agent specialization, combined with semantic clustering, can effectively resolve gradient conflicts and guide prompt optimization toward more robust improvements.
- **Contributions of HCGC and CAAW.** The ablation study confirms that both proposed modules are indispensable. Removing HCGC reduces the ability to enforce semantic compactness and separation, leading to less stable optimization. Disabling CAAW degrades robustness by failing to downweight weaker agents. When both modules are removed, MAPGD collapses close to single-agent performance, highlighting their complementary roles.
- **Efficiency in token usage.** Despite employing multiple agents, MAPGD achieves lower overall token consumption and fewer API calls than ProTeGi. This efficiency stems from clustering redundant gradients and adaptively weighting agents, which reduce unnecessary evaluations. As a result, MAPGD achieves over 10% higher performance-per-token

efficiency, indicating that it not only improves accuracy but also makes more economical use of query budgets.

• **Robustness across tasks.** The improvements are consistent across datasets of varying size, domain, and language, suggesting that MAPGD generalizes well to heterogeneous NLP tasks. Furthermore, the case study in the Appendix illustrates its applicability to open-ended generation, extending beyond controlled classification benchmarks.

• **Transferability to reasoning tasks.** MAPGD also demonstrates strong performance on arithmetic reasoning datasets, surpassing competitive baselines such as PromptWizard. Its consistent improvements on GSM8k, AQUARAT, and SVAMP highlight that the proposed gradient-inspired multi-agent optimization is not limited to classification, but can effectively enhance chain-of-thought style reasoning as well.

In summary, these insights show that MAPGD achieves a favorable balance between performance and efficiency, while its modular design (HCGC + CAAW) provides both effectiveness and robustness in diverse prompt optimization scenarios.

5 DISCUSSION

MAPGD advances prompt optimization by combining gradient-inspired reasoning with multi-agent collaboration. Its two key mechanisms—Hypersphere-Constrained Gradient Clustering and Channel-Adaptive Agent Weighting enable more structured, interpretable, and efficient optimization.

Modularity. By separating gradient generation, clustering, weighting, and candidate selection, MAPGD clarifies which components drive performance, supporting transparent analysis and principled extensions.

Conflict resolution. HCGC enforces angular margin constraints on the hypersphere, promoting intra-cluster compactness and inter-cluster separation. This directly addresses conflicts among agent-generated gradients, common in tasks such as fake news detection or jailbreak classification, and parallels gradient surgery in multi-task learning but for discrete prompts.

Adaptive collaboration. CAAW allocates influence based on agent reliability, reducing noise from weaker gradients while amplifying consistent signals. This is useful when tasks emphasize different reasoning dimensions (e.g., semantic consistency vs. contextual grounding).

Budget-awareness. With lightweight bandit-based selection, MAPGD improves performance-per-token efficiency, achieving higher accuracy with fewer redundant API calls.

Limitations. MAPGD depends on embedding quality and agent reliability; under strong domain shifts, clustering may be unstable and weighting may amplify spurious signals. Future work may strengthen semantic representations and improve agent calibration.

Future directions. Promising avenues include:

- (1) Cross-task generalization: training reusable agents with transferable clustering and weighting behaviors.
- (2) Human-in-the-loop fusion: leveraging expert oversight to guide clustering and validate weighting.

- (3) Hybrid optimization: integrating MAPGD with differentiable prompt tuning to balance interpretability and efficiency.

6 CONCLUSION

We presented MAPGD: Multi-Agent Prompt Gradient Descent, a novel framework for optimizing prompts in large language models. The key innovations of MAPGD are HCGC, which resolves conflicts through hypersphere-constrained clustering, and CAAW, which adaptively balances the contributions of specialized agents. Together, these mechanisms enable diverse agents to collaborate effectively while maintaining semantic alignment.

Empirically, MAPGD achieves consistent improvements over strong baselines such as ProTeGi, Monte Carlo search, reinforcement learning-based methods, and recent arithmetic reasoning frameworks. On four benchmark classification tasks, MAPGD improves F1 scores by 3–7% on average while reducing token consumption by ~8%, leading to better performance-per-token efficiency. Beyond classification, MAPGD also demonstrates strong transferability to arithmetic reasoning datasets such as GSM8k, AQUARAT, and SVAMP, where it surpasses competitive baselines including PromptWizard. These results confirm that gradient-inspired multi-agent collaboration is broadly applicable across both discriminative and reasoning tasks.

Theoretically, we show that MAPGD achieves a sublinear convergence rate of $O(1/\sqrt{T})$ under standard stochastic approximation assumptions (see Appendix C for details). This result indicates that even in a discrete prompt space, the semantic gradient mechanism—stabilized by HCGC and CAAW—retains the efficiency of classical stochastic gradient descent.

While challenges remain, particularly regarding embedding robustness and LLM feedback reliability, MAPGD provides both a practical toolkit for efficient prompt optimization and a theoretical foundation linking discrete semantic updates with continuous optimization theory. Future work may extend HCGC and CAAW to multimodal prompts, incorporate human preference alignment, and develop cross-domain reusable agents.

In summary, MAPGD demonstrates that multi-agent collaboration, when combined with principled clustering and adaptive weighting, leads to more robust, interpretable, and resource-efficient prompt optimization, with demonstrated effectiveness across classification, reasoning, and beyond.

REFERENCES

[1] Josh Achiam, Steven Adler, Sandhini Agarwal, Lama Ahmad, Ilge Akkaya, Florencia Leoni Aleman, Diogo Almeida, Janko Altenschmidt, Sam Altman, Shyamal Anadkat, et al. 2023. Gpt-4 technical report. *arXiv preprint arXiv:2303.08774* (2023).

[2] Eshaan Agarwal, Joykiran Singh, Vivek Dani, Raghav Magazine, Tanuja Ganu, and Akshay Nambi. 2024. PromptWizard: Task-Aware Prompt Optimization Framework. *arXiv:2405.18369 [cs.CL]* <https://arxiv.org/abs/2405.18369>

[3] Jean-Yves Audibert and Sébastien Bubeck. 2010. Best arm identification in multi-armed bandits. In *COLT-23th Conference on learning theory-2010*. 13–p.

[4] Sébastien Bubeck, Varun Chandrasekaran, Ronen Eldan, Johannes Gehrke, Eric Horvitz, Ece Kamar, Peter Lee, Yin Tat Lee, Yuanzhi Li, Scott Lundberg, et al. 2023. Sparks of artificial general intelligence: Early experiments with gpt-4. *arXiv preprint arXiv:2303.12712* (2023).

[5] Lichang Chen, Juhai Chen, Tom Goldstein, Heng Huang, and Tianyi Zhou. 2023. InstructZero: Efficient Instruction Optimization for Black-Box Large Language Models. *arXiv:2306.03082 [cs.AI]* <https://arxiv.org/abs/2306.03082>

[6] Shuo Chen, Gang Niu, Chen Gong, Jun Li, Jian Yang, and Masashi Sugiyama. 2021. Large-margin contrastive learning with distance polarization regularizer. In *International conference on machine learning*. PMLR, 1673–1683.

[7] Karl Cobbe, Vineet Kosaraju, Mohammad Bavarian, Mark Chen, Heewoo Jun, Lukasz Kaiser, Matthias Plappert, Jerry Tworek, Jacob Hilton, Reichiro Nakano, et al. 2021. Training verifiers to solve math word problems. *arXiv preprint arXiv:2110.14168* (2021).

[8] Jiankang Deng, Jia Guo, Niannan Xue, and Stefanos Zafeiriou. 2019. Arcface: Additive angular margin loss for deep face recognition. In *Proceedings of the IEEE/CVF conference on computer vision and pattern recognition*. 4690–4699.

[9] Mingkai Deng, Jianyu Wang, Cheng-Ping Hsieh, Yihan Wang, Han Guo, Tianmin Shu, Meng Song, Eric P Xing, and Zhiting Hu. 2022. Rlprompt: Optimizing discrete text prompts with reinforcement learning. *arXiv preprint arXiv:2205.12548* (2022).

[10] Yilun Du, Shuang Li, Antonio Torralba, Joshua B Tenenbaum, and Igor Mordatch. 2023. Improving factuality and reasoning in language models through multiagent debate. In *Forty-first International Conference on Machine Learning*.

[11] Ibrahim Abu Farha and Walid Magdy. 2020. From arabic sentiment analysis to sarcasm detection: The arsarcasm dataset. In *The 4th Workshop on Open-Source Arabic Corpora and Processing Tools*. European Language Resources Association (ELRA), 32–39.

[12] Chrisantha Fernando, Dylan Banarse, Charles Blundell, Tim Rocktäschel, and Simon Osindero. 2023. PromptBreeder: Self-Referential Self-Improvement Via Prompt Evolution. *arXiv preprint arXiv:2309.16797* (2023).

[13] Sirui Hong, Mingchen Zhuge, Jiaqi Chen, Xiawu Zheng, Yuheng Cheng, Ceyao Zhang, Jinlin Wang, Zili Wang, Steven Ka Shing Yau, Zijuan Lin, Liyang Zhou, Chenyu Ran, Lingfeng Xiao, Chenglin Wu, and Jürgen Schmidhuber. 2024. MetaGPT: Meta Programming for A Multi-Agent Collaborative Framework. *arXiv:2308.00352 [cs.AI]* <https://arxiv.org/abs/2308.00352>

[14] Jie Hu, Li Shen, and Gang Sun. 2018. Squeeze-and-excitation networks. In *Proceedings of the IEEE conference on computer vision and pattern recognition*. 7132–7141.

[15] Ellen Jiang, Kristen Olson, Edwin Toh, Alejandra Molina, Aaron Donsbach, Michael Terry, and Carrie J Cai. 2022. Promptmaker: Prompt-based prototyping with large language models. In *CHI Conference on Human Factors in Computing Systems Extended Abstracts*. 1–8.

[16] Brian Lester, Rami Al-Rfou, and Noah Constant. 2021. The power of scale for parameter-efficient prompt tuning. *arXiv preprint arXiv:2104.08691* (2021).

[17] Xiang Li and Percy Liang. 2021. Prefix-Tuning: Optimizing Continuous Prompts for Generation. *Proceedings of the 59th Annual Meeting of the Association for Computational Linguistics and the 11th International Joint Conference on Natural Language Processing (Volume 1: Long Papers)* (2021), 4582–4597. <https://api.semanticscholar.org/CorpusID:230433941>

[18] Weizhe Liang, Yizhong Wu, Mina Lee, Ed Chi, Denny Zhou, Yiming Song, and Xiang Li. 2023. Encouraging Divergent Thinking in Large Language Models through Multi-Agent Debate. *arXiv preprint arXiv:2305.19118* (2023).

[19] Xiaoqiang Lin, Zhaoxuan Wu, Zhongxiang Dai, Wenyang Hu, Yao Shu, See-Kiong Ng, Patrick Jaillet, and Bryan Kian Hsiang Low. 2024. Use Your INSTINCT: INSTRUCTION optimization for LLMs using Neural bandits Coupled with Transformers. *arXiv:2310.02905 [cs.LG]* <https://arxiv.org/abs/2310.02905>

[20] Wang Ling, Dani Yogatama, Chris Dyer, and Phil Blunsom. 2017. Program induction by rationale generation: Learning to solve and explain algebraic word problems. *arXiv preprint arXiv:1705.04146* (2017).

[21] Weiyang Liu, Yandong Wen, Zhiding Yu, Ming Li, Bhiksha Raj, and Le Song. 2017. Sphereface: Deep hypersphere embedding for face recognition. In *Proceedings of the IEEE conference on computer vision and pattern recognition*. 212–220.

[22] Ioannis Mollas, Zoe Chrysopoulou, Stamatis Karlos, and Grigoris Tsoumacas. 2022. ETHOS: a multi-label hate speech detection dataset. *Complex & Intelligent Systems* 8, 6 (2022), 4663–4678.

[23] Arkil Patel, Satwik Bhattacharya, and Navin Goyal. 2021. Are NLP models really able to solve simple math word problems? *arXiv preprint arXiv:2103.07191* (2021).

[24] Archiki Prasad, Peter Hase, Xiang Zhou, and Mohit Bansal. 2022. Grips: Gradient-free, edit-based instruction search for prompting large language models. *arXiv preprint arXiv:2203.07281* (2022).

[25] Reid Pryzant, Dan Iter, Jerry Li, Yin Tat Lee, Chenguang Zhu, and Michael Zeng. 2023. Automatic prompt optimization with “gradient descent” and beam search. *arXiv preprint arXiv:2305.03495* (2023).

[26] Guanghui Qin and Jason Eisner. 2021. Learning how to ask: Querying LMs with mixtures of soft prompts. *arXiv preprint arXiv:2104.06599* (2021).

[27] Laria Reynolds and Kyle McDonnell. 2021. Prompt programming for large language models: Beyond the few-shot paradigm. In *Extended abstracts of the 2021 CHI conference on human factors in computing systems*. 1–7.

[28] Pranab Sahoo, Ayush Kumar Singh, Sriparna Saha, Vinija Jain, Samrat Mondal, and Aman Chadha. 2025. A Systematic Survey of Prompt Engineering in Large Language Models: Techniques and Applications. *arXiv:2402.07927 [cs.AI]* <https://arxiv.org/abs/2402.07927>

[29] Xinyue Shen, Zeyuan Chen, Michael Backes, Yun Shen, and Yang Zhang. 2024. “do anything now”: Characterizing and evaluating in-the-wild jailbreak prompts on large language models. In *Proceedings of the 2024 on ACM SIGSAC Conference on Computer and Communications Security*. 1671–1685.

[30] Taylor Shin, Yasaman Razeghi, Robert L Logan IV, Eric Wallace, and Sameer Singh. 2020. Autoprompt: Eliciting knowledge from language models with automatically generated prompts. *arXiv preprint arXiv:2010.15980* (2020).

[31] Hao Wang, Yitong Wang, Zheng Zhou, Xing Ji, Dihong Gong, Jingchao Zhou, Zhifeng Li, and Wei Liu. 2018. Cosface: Large margin cosine loss for deep face recognition. In *Proceedings of the IEEE conference on computer vision and pattern recognition*. 5265–5274.

[32] Tongzhou Wang and Phillip Isola. 2020. Understanding contrastive representation learning through alignment and uniformity on the hypersphere. In *International conference on machine learning*. PMLR, 9929–9939.

[33] W Wang. 2021. A new benchmark dataset for fake news detection. In *Proceedings of the 55th Annual Meeting of the Association for Computational Linguistics, Vol. 2*.

[34] Jinyu Xiang, Jiayi Zhang, Zhaoyang Yu, Xinbing Liang, Fengwei Teng, Jinhao Tu, Fashen Ren, Xiangru Tang, Sirui Hong, Chenglin Wu, and Yuyu Luo. 2025. Self-Supervised Prompt Optimization. *arXiv:2502.06855 [cs.CL]* <https://arxiv.org/abs/2502.06855>

[35] J Diego Zamfirescu-Pereira, Richmond Y Wong, Bjoern Hartmann, and Qian Yang. 2023. Why Johnny can’t prompt: how non-AI experts try (and fail) to design LLM prompts. In *Proceedings of the 2023 CHI conference on human factors in computing systems*. 1–21.

[36] Tianjiao Zhang, Xuezhi Wang, Denny Zhou, Dale Schuurmans, and Joseph E Gonzalez. 2022. Tempera: Test-time prompting via reinforcement learning. *arXiv preprint arXiv:2211.11890* (2022).

[37] Yongchao Zhou, Andrei Ioan Muresanu, Ziwen Han, Keiran Paster, Silvia Pitis, Harris Chan, and Jimmy Ba. 2022. Large language models are human-level prompt engineers. In *The eleventh international conference on learning representations*.

A CAAW PARAMETER SENSITIVITY

The Channel-Adaptive Agent Weighting module uses a temperature parameter λ to control the emphasis on historically effective agents during gradient fusion. To evaluate the robustness of MAPGD with respect to λ , we conducted experiments on two representative datasets: **LIAR**(binary) and **GSM8K** (mathematical reasoning).

We tested three values of λ : 0.5, 1, and 2. Table 4 summarizes the test accuracy for each setting. The results indicate that moderate variations of λ do not significantly affect the overall performance, supporting the choice of $\lambda = 1$ in the main experiments.

Table 4: Test accuracy of MAPGD under different CAAW weighting parameter λ . Performance differences are minor, demonstrating robustness to λ .

λ	LIAR Accuracy	GSM8K Accuracy
0.5	0.709	0.927
1	0.717	0.935
2	0.711	0.933

As shown in Table 4, the test accuracy exhibits only minor variations across the three λ values, with a maximum difference of 0.008 on LIAR and 0.008 on GSM8K. These variations are small relative to the overall performance gains achieved by multi-agent gradient fusion, indicating that while λ influences the sharpness of agent weighting, MAPGD’s performance remains stable for reasonable choices around the default setting of $\lambda = 1$.

B COMPLEXITY AND PARALLELISM

The computational bottleneck of MAPGD with HCGC and CAAW (see Algorithm 1) lies in LLM calls for gradient generation, cluster fusion, and prompt expansion, whereas embedding, clustering, similarity checks, and adaptive weighting involve comparatively lightweight vector operations. Multi-agent parallelization significantly reduces wall time, making the framework scalable for practical deployment. In the following, we analyze the per-iteration computational and memory costs, providing a detailed breakdown of the dominant operations and their respective complexities.

Notation. Let N be the number of agents, m the number of reasons per agent, giving $G = Nm$ atomic gradients. Embedding dimension d , clusters $K \leq G$, fused gradients $|\tilde{\mathcal{G}}|$, expansion variants per gradient s , MC paraphrases per variant n_{mc} , candidate prompts $|C|$, beam width k , bandit rounds T_b with K_{eval} arms and dev mini-batch size b .

Stage costs (time).

- (1) **Agent gradient generation:** Each of the N agents generates m gradients using LLMs, giving $O(N)$ LLM calls. Parallelization reduces wall time to $\approx \max t_{\text{LLM}}$.
- (2) **HCGC embedding + conflict detection:** Embedding each gradient costs $O(Gd)$; computing pairwise angular conflicts costs $O(G^2d)$. For small G (e.g., $G \sim 16$), this is negligible compared with LLM calls.
- (3) **HCGC clustering:** KMeans clustering over G gradients into K clusters with I iterations costs $O(GKId)$, again minor due to small G .
- (4) **HCGC fusion (LLM):** Clusters with multiple gradients require one LLM call per cluster to fuse into a coherent gradient. Total LLM calls up to $O(K_{\text{merge}})$, parallelizable across clusters.
- (5) **CAAW weighting and fusion:** Per-cluster adaptive weighting is $O(G)$ vector operations, negligible compared to LLM fusion.
- (6) **Prompt expansion + MC paraphrasing:** Applying each fused gradient: $O(|\tilde{\mathcal{G}}|)$ gradient applications. MC paraphrasing for each variant: $O(|\tilde{\mathcal{G}}|sn_{mc})$ LLM calls.
- (7) **Diversity filtering:** Computing embeddings: $O(|C|d)$; naive pairwise similarities: $O(|C|^2)$. For tens of candidate prompts, this remains negligible.
- (8) **Bandit evaluation:** Probing K_{eval} arms over mini-batches of size b for T_b rounds: $O(K_{\text{eval}}bT_b)$, significantly cheaper than exhaustive evaluation $O(|C||D_{\text{dev}}|)$.

Space complexity. Text storage: $O(|C|L_{\text{avg}})$. Embeddings: $O((G+|C|)d)$, typically a few MB. Optional caches (unique prompts or intermediate LLM outputs) scale linearly with the number of prompts and clusters.

Algorithm 1 MAPGD with HCGC and CAAW

Require: Initial prompt p_0 , train data D_{train} , dev data D_{dev} , agents $\{A_i\}_{i=1}^N$, iterations R , beam width k

- 1: Initialize best prompt $p_{\star}^{(0)} \leftarrow p_0$, beam $B_0 \leftarrow \{p_0\}$; initialize each agent prompt $A_i.p \leftarrow p_0$
- 2: **for** $t = 1$ to R **do**
- 3: $M_t \leftarrow \text{SAMPLEMINIBATCH}(D_{\text{train}}, b)$
- 4: $\mathcal{G}_t \leftarrow \text{GENERATEAGENTGRADIENTS}(\{A_i\}, M_t)$ ▷ Alg. 2
- 5: $\tilde{\mathcal{G}}_t \leftarrow \text{HCGC}(\mathcal{G}_t)$ ▷ Alg. 3
- 6: $F_t \leftarrow \text{CAAWFUSE}(\tilde{\mathcal{G}}_t, D_{\text{dev}})$ ▷ Alg. 4
- 7: $C_t \leftarrow \text{EXPANDPROMPTS}(p_{\star}^{(t-1)}, F_t)$
- 8: $B_t, p_{\star}^{(t)} \leftarrow \text{BANDITSELECT}(C_t, D_{\text{dev}}, k)$
- 9: $\text{SYNCHRONIZEAGENTS}(\{A_i\}, p_{\star}^{(t)})$ ▷ Alg. 5
- 10: **if** $\text{CONVERGED}(p_{\star}^{(t)})$ **then break**
- 11: **end if**
- 12: **end for**
- 13: **return** Best prompt over $\{p_{\star}^{(1)}, \dots, p_{\star}^{(t)}\}$

Algorithm 2 Multi-Agent Textual Gradient Generation

Require: Agents $\{A_i\}$, mini-batch M_t , task T , predictor Π , per-agent error cap e , feedback count m

- 1: **for all** agent A_i in parallel **do**
- 2: (\hat{y}, y) pairs $\leftarrow T.\text{INFERANDLABEL}(A_i.p, M_t, \Pi)$
- 3: $E_i \leftarrow \text{SELECTERRORS}(\hat{y}, y, e)$
- 4: **if** $|E_i| = 0$ **then** $E_i \leftarrow \text{DIVERSESAMPLES}(M_t, e)$
- 5: **end if**
- 6: $\text{raw}_i \leftarrow \text{LLMGRADIENTPROMPT}(A_i.\text{role}, A_i.p, E_i, m)$
- 7: $g_i \leftarrow \text{PARSEGRADIENTBLOCKS}(\text{raw}_i)$ ▷ Split by delimiters
- 8: **end for**
- 9: **return** $\mathcal{G}_t = \{(A_i.\text{role}, g_i)\}_{i=1}^N$

Algorithm 3 Hypersphere-Constrained Gradient Clustering

Require: Agent gradients \mathcal{G}_t

- 1: Embed and normalize: $\hat{v}_k = \phi(g_k)/\|\phi(g_k)\|$
- 2: Detect conflicts: $C_{\text{conf}} \leftarrow \{(i, j) : \cos^{-1}(\hat{v}_i^T \hat{v}_j) > \theta\}$
- 3: Cluster gradients: $\{S_k\}_{k=1}^K \leftarrow \text{KMEANS}(\{\hat{v}_k\}, K_{\text{max}})$
- 4: **for** $k = 1$ to K **do**
- 5: Apply angular margin: reassign gradients violating $\cos(n \cdot \Delta(\hat{v}_i, c_k)) > \cos(\Delta(\hat{v}_i, c_j))$
- 6: Fuse cluster S_k via LLM: $f_k \leftarrow \text{LLMFUSE}(S_k, C_{\text{conf}})$
- 7: **end for**
- 8: **return** Fused clusters: $\tilde{\mathcal{G}}_t = \{f_1, \dots, f_K\}$

C THEORETICAL ANALYSIS

In this section, we provide convergence guarantees for MAPGD under mild assumptions, following the stochastic approximation framework. Our goal is to bridge the gap between the continuous optimization theory of stochastic gradient descent (SGD) and the discrete prompt optimization carried out in MAPGD. We show that, despite operating in a structured and discrete search space, MAPGD achieves the same sublinear convergence rate of $O(1/\sqrt{T})$ in both convex and non-convex settings.

Algorithm 4 Channel-Adaptive Agent Weighting and Fusion

Require: Clustered gradients $\tilde{\mathcal{G}}_t$, dev data D_{dev} , temperature λ

- 1: **for all** cluster $\tilde{\mathcal{G}}_t$ **do**
- 2: Compute per-gradient validation gain s_i on D_{dev}
- 3: Assign adaptive weight: $w_i = \frac{\exp(\lambda s_i)}{\sum_{j \in S_k} \exp(\lambda s_j)}$
- 4: Fuse cluster gradients: $f_k = \Psi\left(\sum_{i \in S_k} w_i g_i\right)$
- 5: **end for**
- 6: **return** $F_t = \{f_1, \dots, f_K\}$

Algorithm 5 SynchronizeAgents

Require: Agents $\{A_i\}_{i=1}^N$, current best prompt $p_{\star}^{(t)}$

- 1: **for each agent** A_i **do**
- 2: $A_i.p \leftarrow p_{\star}^{(t)}$ \triangleright Set the agent's current prompt to the global best
- 3: RESETGRADIENTHISTORY(A_i) \triangleright Optional: clear outdated gradient history
- 4: UPDATEPERFORMANCEMEMORY($A_i, p_{\star}^{(t)}$) \triangleright Record performance feedback for the new prompt
- 5: **end for**
- 6: **return** Updated agents $\{A_i\}$

C.1 Assumptions

We begin with a set of assumptions standard in stochastic optimization but reinterpreted in the context of multi-agent prompt optimization.

- **(A1) Alignment (Unbiasedness).** For some $\mu > 0$, the stochastic semantic gradient $g^{(t)}$ maintains alignment with the true gradient:

$$\mathbb{E}[\langle g^{(t)}, \nabla F(p^{(t)}) \rangle \mid p^{(t)}] \geq \mu \|\nabla F(p^{(t)})\|^2.$$

This reflects the role of semantic fusion: multi-agent aggregation reduces the chance of adversarial or noisy updates, ensuring progress along descent directions.

- **(A2) Bounded Second Moment.** For constants $\rho, \sigma^2 \geq 0$,

$$\mathbb{E}[\|g^{(t)}\|^2 \mid p^{(t)}] \leq \rho \|\nabla F(p^{(t)})\|^2 + \sigma^2.$$

This captures the variance-control effect of the bandit-based selection mechanism, which prevents uncontrolled explosion of gradient magnitude.

- **(A3) Smoothness or Lipschitzness.** For convex tasks, F is G -Lipschitz with domain diameter D . For non-convex tasks, F is L -smooth: $\|\nabla F(u) - \nabla F(v)\| \leq L\|u - v\|$.

C.2 Supporting Lemmas

We restate two standard lemmas, adapted to the MAPGD setting.

Lemma 1 (Convex Projection Inequality). For convex F with feasible set \mathcal{P} , the projected subgradient update

$$p^{(t+1)} = \Pi_{\mathcal{P}}(p^{(t)} - \eta g^{(t)})$$

satisfies

$$\|p^{(t+1)} - p^*\|^2 \leq \|p^{(t)} - p^*\|^2 - 2\eta \langle g^{(t)}, p^{(t)} - p^* \rangle + \eta^2 \|g^{(t)}\|^2.$$

Lemma 2 (Non-Convex Descent Lemma). If F is L -smooth, then for update $p^{(t+1)} = p^{(t)} - \eta g^{(t)}$, we have

$$F(p^{(t+1)}) \leq F(p^{(t)}) - \eta \langle \nabla F(p^{(t)}), g^{(t)} \rangle + \frac{L}{2} \eta^2 \|g^{(t)}\|^2.$$

C.3 Main Results

Convex Convergence. Suppose F is convex, G -Lipschitz, and \mathcal{P} has diameter D . Let $\bar{p}_T = \frac{1}{T} \sum_{t=1}^T p^{(t)}$. Under (A1)–(A2) and step size $\eta = \frac{D}{G\sqrt{T}}$, we obtain:

$$\mathbb{E}[F(\bar{p}_T)] - F(p^*) = O\left(\frac{1}{\sqrt{T}}\right).$$

Proof sketch. By Lemma 1 and convexity:

$$F(p^{(t)}) - F(p^*) \leq \langle g^{(t)}, p^{(t)} - p^* \rangle.$$

Summing over $t = 1, \dots, T$ and applying (A1)–(A2), we bound the regret:

$$\sum_{t=1}^T \mathbb{E}[F(p^{(t)}) - F(p^*)] \leq \frac{D^2}{2\eta} + \frac{\eta G^2 T}{2}.$$

Using Jensen's inequality for \bar{p}_T and optimizing η , we conclude the $O(1/\sqrt{T})$ rate.

Non-Convex Convergence. Suppose F is L -smooth and (A1)–(A2) hold. With constant step size $\eta = \Theta(1/\sqrt{T})$, we have

$$\frac{1}{T} \sum_{t=1}^T \mathbb{E}[\|\nabla F(p^{(t)})\|^2] = O\left(\frac{1}{\sqrt{T}}\right).$$

Proof sketch. Applying Lemma 2 and taking conditional expectation:

$$\begin{aligned} \mathbb{E}[F(p^{(t+1)})] &\leq \mathbb{E}[F(p^{(t)})] - \eta \mu \mathbb{E}[\|\nabla F(p^{(t)})\|^2] \\ &\quad + \frac{L}{2} \eta^2 \left(\rho \mathbb{E}[\|\nabla F(p^{(t)})\|^2] + \sigma^2 \right). \end{aligned} \quad (10)$$

Summing over $t = 1 \dots T$ gives

$$\frac{1}{T} \sum_{t=1}^T \mathbb{E}[\|\nabla F(p^{(t)})\|^2] \leq \frac{2(F(p^{(1)}) - F_{\inf})}{\mu T \eta} + \frac{L \sigma^2}{\mu} \eta.$$

Balancing terms with $\eta = \Theta(1/\sqrt{T})$ yields the claimed rate.

C.4 Summary of Theoretical Guarantees

In this work, we bridge the gap between classical stochastic optimization, which assumes continuous parameter spaces, and the inherently discrete, structured nature of prompt optimization. Our convergence analysis for MAPGD does not require the discrete prompt space to be continuous. Instead, we show that the framework's core mechanisms ensure that the optimization process satisfies the key conditions of stochastic approximation theory.

The argument unfolds along three main dimensions:

- **Directional Alignment (A1):** Although textual pseudo-gradients are not true mathematical gradients, Hypersphere-Constrained Gradient Clustering aggregates semantically coherent suggestions from multiple agents into a fused gradient that statistically aligns with the true descent direction.

- **Variance Control (A2):** Discrete prompt edits are prone to high variance, but the bandit-based candidate selection mechanism filters out unreliable or detrimental candidates. This effectively bounds the second moment of stochastic updates.
- **Smoothness Justification (A3):** We assume the empirical loss function is Lipschitz or smooth in the semantic embedding space, even though the prompts themselves are discrete.

Given that these conditions are met, MAPGD inherits the convergence guarantees of classical stochastic gradient descent. Consequently, despite operating in a discrete textual space, MAPGD achieves a robust sublinear convergence rate of $O(1/\sqrt{T})$, providing a solid theoretical foundation for the observed empirical effectiveness of our multi-agent, geometry-aware approach to prompt optimization.

D CASE STUDY: SYSTEM PROMPT OPTIMIZATION

To further illustrate the applicability of MAPGD, we present a case study where our method is applied to optimize the system prompt of a large language model assistant. The original prompt is designed to support multi-source analysis and financial data interpretation for decision-making tasks. Using MAPGD, we refine the prompt to enhance robustness, accuracy, and interpretability by embedding explicit verification protocols, structured analysis guidelines, and risk prioritization frameworks. This example highlights how MAPGD can be deployed in practical LLM applications beyond benchmark datasets, particularly in domains where data authenticity, reliability, and interpretability are critical.

Original System Prompt. You are an AI assistant designed to process, analyze, and synthesize information from multiple sources in order to answer user questions, generate insights, and prepare detailed reports. You have specialized capabilities in financial data interpretation, knowledge retrieval, and multi-source analysis. You support both operational and strategic decision-making for Golden Section's portfolio companies.

Optimized System Prompt via MAPGD. You are an AI assistant specialized in processing, analyzing, and synthesizing information from multiple sources to answer user questions, generate insights, and prepare detailed reports. Your core capabilities include financial data interpretation, knowledge retrieval, and multi-source analysis, with a focus on supporting operational and strategic decision-making for Golden Section's portfolio companies.

In performing your duties, you must ensure that all input data undergoes rigorous verification for authenticity, accuracy, and completeness before any analysis is conducted. This includes implementing protocols to validate financial figures, legal terms, and other critical information for alignment with established norms and credible sources. Your process must involve:

- Cross-referencing information from diverse, credible sources to detect and mitigate false, exaggerated, or incomplete data.
- Assessing the reliability of each source, prioritizing primary sources where available.

- Identifying and resolving inconsistencies, ambiguities, or potential misinformation through systematic checks.
- Ensuring all risk assessments and conclusions are based solely on validated and accurate inputs to maintain the integrity of your outputs.

Data Authenticity and Completeness Verification

- Scrutinize contextual cues (e.g., “Context: Section: Payback Period.”) to ensure alignment with expected data types and structures.
- Check for numerical or factual inconsistencies, such as typos (e.g., “11975” instead of “1975”), exaggerations (e.g., “\$22.0M” without supporting context), or missing critical information.
- Validate that all referenced data points are present, logically consistent, and contextually appropriate.
- Flag and document any anomalies for further investigation before proceeding with classification or analysis.

Context Interpretation and Parsing Guidelines

- Carefully interpret and utilize contextual cues, especially in nested or ambiguous contexts (e.g., “Context: Section: Name & Headquarters.”).
- Accurately parse section headers and contextual clues to prevent misclassification or incomplete analysis in multi-section reports.
- Anchor analysis to the document’s structure by adhering to hierarchical or sequential organization.
- Resolve discrepancies in contextual labeling or structure to maintain coherence.

Structured Classification and Risk Prioritization Framework

- (1) **Factual Reporting and Descriptive Analysis:** Present verified information such as corporate history, operational metrics, and financial data neutrally, before transitioning to evaluative content.
- (2) **Business Analysis:** Evaluate performance, market positioning, and strategic initiatives; assess risks by severity, likelihood, and propose contextualized mitigation.
- (3) **Legal Risk Analysis:** Examine compliance, regulatory, and contractual risks; assess impact and propose mitigation actions aligned with legal context.
- (4) **Cross-Domain Analysis:** For overlapping elements, classify by primary context and document dual-category cases with rationale.

Validation Mechanisms for Cross-References

- Distinguish between source types (e.g., governance vs. identity records).
- For each statement, explicitly identify the source type and ensure contextual alignment.

Empirical Observation. After applying MAPGD, we observe a notable increase in the comprehensiveness of the generated financial analysis reports. Specifically, the average report length increased from 1616 words under the original system prompt to 1965 words with the optimized prompt. This indicates that the optimized prompt encourages the model to produce more detailed and contextually grounded content. While the per-report output length

becomes longer, the improved accuracy and completeness reduce the need for repeated generations or manual corrections, thereby lowering the overall token consumption in practical workflows. These findings further support that MAPGD enhances the robustness and effectiveness of system prompts in real-world generation tasks.

E AGENT SPECIALIZATION FOR DIFFERENT TASKS

To adapt MAPGD to different domains, we define specialized agent roles tailored to the unique requirements of each task. Below are the agent configurations used for the classification, mathematical reasoning, and financial analysis tasks in our experiments.

E.1 Agent Roles for Classification Tasks

For general classification tasks, the agents focus on the core components of a good prompt: instructions, examples, format, and style.

instruction_specialist Analyzes and improves task instructions, ensuring clarity, completeness, and executability.

example_curator Focuses on selecting representative, diverse examples and ensuring consistent formatting.

format_designer Designs clear output templates and structured formats for better model understanding.

style_optimizer Optimizes language expression for professionalism and task-specific adaptation.

E.2 Agent Roles for Mathematical Reasoning Tasks

For mathematical reasoning, the agent roles are adapted to focus on logical decomposition, calculation, and problem interpretation.

reasoning_specialist Specializes in enhancing mathematical reasoning processes, ensuring clear step-by-step logic and proper problem decomposition.

calculation_optimizer Focuses on improving calculation accuracy, suggesting better computational methods, and ensuring numerical correctness.

problem_interpreter Specializes in interpreting math word problems, extracting relevant information, and identifying mathematical relationships.

solution_formatter Optimizes mathematical solution presentation, ensures clear formatting and proper answer notation (e.g., ##### [final_answer]).

E.3 Agent Roles for Financial Report Analysis

For the complex task of business and financial analysis, agents are given highly specialized roles focusing on data verification, structured report generation, and professional tone.

instruction_specialist Crafts clear, executable instructions for generating truthful, structured reports and rejecting false or exaggerated inputs. Instructions must include steps to verify input data authenticity (e.g., checking financial metrics for realism).

example_curator Selects and formats diverse examples that demonstrate truthful report generation and false data rejection, including both positive (realistic) and negative (exaggerated) samples.

format_designer Specializes in designing clear, structured output templates for reports (e.g., using <Business Analysis>, <Financial Report> tags) and error messages (e.g., <Error>).

style_optimizer Optimizes language style and tone for generating professional reports in business, financial, and legal contexts, while ensuring error messages are direct and unambiguous.

F EXAMPLE PROMPTS BEFORE AND AFTER OPTIMIZATION

This appendix provides the initial prompts and the final optimized prompts generated by MAPGD for each of the benchmark datasets used in our experiments.

F.1 LIAR Dataset

Initial Prompt.

Task

Determine whether the Statement is a lie (Yes) or not (No) based on the Context and other information.

Output format

Answer Yes or No as labels

Prediction

Text: {text}

label:

Optimized Prompt.

Task

Your task is to evaluate the given Statement in the context of the provided information. If the Statement is found to be intentionally false or misleading, it should be classified as a lie. In this case, your response should be 'Yes'. If the Statement is true or unintentionally false due to a mistake or lack of knowledge, it should not be classified as a lie. In this case, your response should be 'No'.

Output format

Provide your answer as 'Yes' or 'No' labels. 'Yes' indicates that the statement is a lie, while 'No' indicates that the statement is not a lie.

Prediction

Text: {text}

label:

F.2 Ethos Dataset

Initial Prompt.

Task

Is the following text hate speech?

Output format

Answer Yes or No as labels

Prediction

Text: {text}

Label:

Optimized Prompt.

Task

Your task is to analyze the following text and determine if it contains hate speech. For the purpose of this task, hate speech is defined as any speech, gesture, conduct, writing, or display that may incite violence or prejudicial actions against or by a protected individual or group, or because it disparages or intimidates a protected individual or group.

Please base your judgment on the explicit content of the text, rather than personal interpretations or assumptions.

Output format

Provide your answer in a clear format as either 'Contains Hate Speech' or 'Does Not Contain Hate Speech'

Prediction

Text: {text}

Label:

F.3 Jailbreak Dataset

Initial Prompt.

Task

Detect if the message is a jailbreak attack, i.e. an attempt by a user to break through an AI system's protections

Output format

Answer Yes or No as labels

Prediction

Text: {text}

Label:

Optimized Prompt.

Task

Classify the message as one of the following labels based on its potential to be a jailbreak attack, i.e., an attempt to bypass an AI system's protections:

- "OvertAttack": The message contains clear, direct attempts to break through system safeguards.
- "SuspiciousContext": The message shows indirect or contextual cues that may indicate a multi-stage or sophisticated attack attempt.
- "Benign": The message poses no apparent risk and does not attempt to circumvent protections.

Output format

Select and output exactly one label from the options above.

Prediction

Text: {text}

Label:

F.4 GSM8K Dataset

Initial Prompt.

Task

Solve the math word problem step by step.

Instructions

1. Read the problem carefully
2. Identify what needs to be calculated

3. Show your work step by step

4. Provide the final numerical answer

Output Format

Show your reasoning process and end with: ##### [final_answer]

Problem

{text}

Optimized Prompt.

Task

Solve the math word problem step by step.

Instructions

1. Read the problem carefully
2. Identify what needs to be calculated
3. If there are ambiguous situations in the problem, make reasonable assumptions and state them clearly
4. Show your work step by step
5. Provide the final numerical answer

Output Format

Show your reasoning process, including any assumptions made, and end with: ##### [final_answer]

Problem

{text}

F.5 AQUARAT Dataset

Initial Prompt.

Task

Solve the math word problem and choose the correct answer from the given options.

Instructions

1. Read the problem carefully
2. Analyze each option
3. Show your reasoning step by step
4. Select the correct answer (A, B, C, D, or E)

Output Format

Show your reasoning and end with: Answer: [LETTER]
(For example: "Answer: A" or "Answer: B")

Problem

{text}

Options

{options}

Optimized Prompt.

Task

Solve the provided problem by systematically classifying its type, analyzing all constraints, applying formal mathematical reasoning, and verifying the solution against all conditions before selecting the correct answer.

Instructions

Adhere strictly to the following structured framework:

1. **Problem Classification:**

* Explicitly identify the core problem domain (e.g.,

"Combinatorial Selection," "Constraint Satisfaction," "Partnership Profit-Sharing," "Work Rate").

- * Justify the classification with a brief rationale based on the problem statement.

2. ****Constraint Analysis:****

- * Enumerate all explicit constraints from the problem text.
- * Infer and list any implicit constraints or logical dependencies.
- * Categorize each constraint (e.g., Hard/Must-Fulfill, Soft/Optimization) and specify their logical relationships (e.g., AND, OR).

3. ****Mathematical Formalization & Numerical Context Resolution:****

- * Identify and resolve any ambiguous numerical references (e.g., "monthly" vs. "annual", "together" vs. "individual").
- * Infer and incorporate any implicit numerical variables (e.g., initial quantities, unstated rates, starting points).
- * Normalize all units to a consistent basis for calculation.
- * Define all variables, sets, and parameters using clear notation (e.g., C_{total} , P_A , $S_{eligible}$, nCr).
- * Structure the problem using appropriate formalisms: timelines, sets, equations, or logical statements.
- * For combinatorial problems, explicitly state the formula used.

4. ****Solution Execution:****

- * Perform all calculations step-by-step, showing substitutions and operations.
- * For combinatorial scenarios, enumerate valid combinations or calculate cardinalities.
- * Derive the target value (e.g., profit share, number of committeees, optimal value).

5. ****Verification & Solution Finalization:****

- * Systematically verify that the proposed solution satisfies every constraint from Step 2.
- * For combinatorial answers, confirm counts against constraints using direct checks or complementary counting.
- * Match the final, verified result to the provided options to select the correct answer.

Output Format

Your final output must follow this structure precisely:

****Problem Classification:****
[Your classification and rationale]

****Constraint**

F.6 SVAMP Dataset

Initial Prompt.

Task
Solve the math word problem step by step.

Instructions

1. Read the problem carefully
2. Identify what needs to be calculated
3. Show your work step by step
4. Provide the final numerical answer

Output Format
Show your reasoning process and end with: ##### [final_answer]

Problem
{text}

Optimized Prompt.

F.7 SVAMP Dataset

Optimized Prompt.

Task
Solve the math word problem through structured, hierarchical reasoning. Your primary goal is to correctly parse and compute multi-step problems involving distinct object categories and their quantitative relationships.

Instructions

1. ****Parse and Categorize:****
Read the problem and question carefully. Identify and list all distinct object types or categories (e.g., 'packages of gum', 'boxes of candy'). For each category, extract:
 - The number of units (e.g., 5 packages).
 - The quantity per unit, if specified (e.g., 8 pieces per package).
2. ****Structure the Solution Hierarchically:****
 - ****Step 1: Calculate Intra-Category Totals.****
For each identified category, calculate its total quantity. If a unit rate is given, perform the multiplication (e.g., $5 \text{ packages} \times 8 \text{ pieces/package} = 40 \text{ pieces of gum}$). If no unit rate exists, use the given quantity directly.
 - ****Step 2: Perform Inter-Category Operations.****
Using the totals from Step 1, now perform the final operation as required by the question (e.g., sum all category totals for a grand total, or find the difference between two category totals for a comparison).
3. ****Show Your Work:****
Present your reasoning clearly, reflecting this two-step hierarchical process. First, show all calculations within categories. Then, show the final combination of these category totals.

4. ****Final Answer:****
Box your final numerical result.

Output Format
Reasoning: [Your step-by-step reasoning here]
[final_answer]

Problem

{text}

Question
{question}